Backleak, tight junctions, and cell- cell adhesion in postischemic injury to the renal allograft.

O Kwon, … , E Alfrey, B D Myers

J Clin Invest. 1998;101(10):2054-2064. https://doi.org/10.1172/JCI772.

Research Article

Postischemic injury in recipients of 3-7-d-old renal allografts was classified into sustained (n = 19) or recovering (n = 20) acute renal failure (ARF) according to the prevailing inulin clearance. Recipients of optimally functioning, long-standing allografts and living donors undergoing nephrectomy served as functional (n = 14) and structural controls (n = 10), respectively. Marked elevation above control of fractional clearance of dextrans of graded size was consistent with transtubular backleak of 57% of filtrate (inulin) in sustained ARF. No backleak was detected in recovering ARF. To explore a structural basis for backleak, allograft biopsies were taken intraoperatively, 1 h after reperfusion in all recipients, and again on day 7 after transplant in a subset (n = 10). Electron microscopy revealed disruption of both apical and basolateral membranes of proximal tubule cells in both sustained and recovering ARF, but cell exfoliation and tubule basement membrane denudation were negligible. Histochemical analysis of membrane-associated adhesion complexes confirmed an abnormality of proximal but not distal tubule cells, marked in sustained ARF but not in recovering ARF. Staining for the zonula occludens complex (ZO-1) and adherens complex (alpha, beta, and gamma catenins) revealed diminished intensity and redistribution of each cytoskeletal protein from the apico-lateral membrane boundary. We conclude that impaired integrity of tight junctions and cell-cell adhesion in the proximal tubule provides a paracellular […]

Backleak, Tight Junctions, and Cell–Cell Adhesion in Postischemic Injury to the Renal Allograft

Osun Kwon,* W. James Nelson,‡ Richard Sibley,§ Philip Huie,§ John D. Scandling,* Donald Dafoe,‖ Edward Alfrey,‖ and Bryan D. Myers*

**Division of Nephrology, ‡Department of Molecular and Cellular Physiology, §Department of Pathology, and ‖Transplant Program, Stanford University School of Medicine, Stanford, California 94305*

Abstract

Postischemic injury in recipients of 3–7-d-old renal allografts was classified into sustained ($n = 19$) or recovering ($n = 20$) acute renal failure (ARF) according to the prevailing inulin clearance. Recipients of optimally functioning, long-standing allografts and living donors undergoing nephrectomy served as functional ($n = 14$) and structural controls ($n = 10$), respectively. Marked elevation above control of fractional clearance of dextrans of graded size was consistent with transtubular backleak of 57% of filtrate (inulin) in sustained ARF. No backleak was detected in recovering ARF. To explore a structural basis for backleak, allograft biopsies were taken intraoperatively, 1 h after reperfusion in all recipients, and again on day 7 after transplant in a subset ($n = 10$). Electron microscopy revealed disruption of both apical and basolateral membranes of proximal tubule cells in both sustained and recovering ARF, but cell exfoliation and tubule basement membrane denudation were negligible. Histochemical analysis of membrane-associated adhesion complexes confirmed an abnormality of proximal but not distal tubule cells, marked in sustained ARF but not in recovering ARF. Staining for the zonula occludens complex (ZO-1) and adherens complex (α, β, and γ catenins) revealed diminished intensity and redistribution of each cytoskeletal protein from the apico-lateral membrane boundary. We conclude that impaired integrity of tight junctions and cell–cell adhesion in the proximal tubule provides a paracellular pathway through which filtrate leaks back in sustained allograft ARF. (*J. Clin. Invest.* 1998. 101:2054–2064.) Key words: fractional dextran clearances • tubule cell pathobiology • zonula occludens • adherens complex • cell-substratum adhesion

Introduction

Postischemic injury to the kidney that manifests as acute renal failure (ARF)[1] is characterized by profound depression of the glomerular filtration rate (GFR). Studies of postischemic ARF in experimental animals that have used the techniques of nephron micropuncture have identified a reduction in filtration pressure, owing to a combination of afferent arteriolar constriction and tubular obstruction, as the major mechanism by which GFR is lowered (1–3). More indirect techniques point also to dissipation of filtration pressure as a principal cause of filtration failure in hemodynamically induced forms of ARF in humans (4–6).

In addition to a reduction of the actual rate at which filtrate is formed, animal models of postischemic ARF are characterized by a reduction in the "effective" GFR, where the latter is defined as the rate at which filtrate is delivered into final urine. This is a consequence of transtubular backleak of a fraction of the filtrate that is formed, a phenomenon that is attributable to a loss of those properties that normally render the tubule cell monolayer impermeable to certain components of filtrate (7–9). Such altered permeability is most readily studied in cultured tubule cell monolayers in vitro and in animal models of postischemic ARF (10–15). Using hypoxia followed by reoxygenation to deplete ATP and simulate ischemia/reperfusion injury in vivo, it has been shown that such injury is associated with striking derangements of the tubule cell cytoskeleton. These include impaired expression of the protein complex responsible for the integrity of intercellular tight junctions and a redistribution of adhesion molecules that are implicated in cell–cell or cell–matrix adhesion (11–15). However, studies of structural/functional defects in these protein complexes in human ARF have not been performed.

In an effort to characterize tubule pathophysiology in a human form of ARF, we have studied the ischemia/reperfusion injury that occurs in the immediate wake of renal allotransplantation. Both tubular and vascular components of the latter injury have been found to resemble strongly postischemic ARF in experimental animals. However, one exception is the absence of morphological evidence of tubular obstruction (4). The present study was thus designed to determine whether transtubular backleak of filtrate contributes to posttransplantation ARF. We used a physiological technique to identify the phenomenon of backleak (16, 17), and combined morphological and histochemical analyses of the tubule cell adhesion complexes in renal allografts to explore potential mechanisms for such backleak. Our findings form the basis of this report.

Methods

Patients

39 patients undergoing transplantation comprised our experimental population. Each gave informed consent to a postoperative study of renal allograft function and structure that had been approved previously by the Committee for Research in Human Subjects at Stanford University. They ranged in age from 28 to 71 yr. The corresponding age range of the donors (of whom 35 were cadaveric and 4 living) was

Address correspondence to Bryan D. Myers, M.D., Division of Nephrology/S201, Stanford University Medical Center, Stanford, CA 94305-5114. Phone: 650-723-6247; FAX: 650-723-7917; E-mail: hf.hht.@forsythe.stanford.edu

Received for publication 30 May 1997 and accepted in revised form 9 March 1998.

1. *Abbreviation used in this paper:* ARF, acute renal failure.

J. Clin. Invest.

0021-9738/98/05/2054/11 $2.00
Volume 101, Number 10, May 1998, 2054–2064
http://www.jci.org

6–65 yr. A determination of effective GFR, as measured by inulin clearance, on days 3–7 after transplant was used to divide the subjects into two groups. Those ($n = 19$) in whom the effective GFR was depressed by two-thirds or more below the normal mean value for an optimally functioning, renal allograft (77 ml/min/1.73 m^2) were classified as sustained ARF. In the remainder ($n = 20$), the effective GFR was depressed by less than two-thirds, and they were classified as recovering ARF.

Two groups of subjects served as controls. 14 long-standing recipients of living donor kidneys that had never undergone rejection served as functional controls. They provided control values for the aforementioned clearance of inulin, as well as for transglomerular sieving of dextran in an optimally functioning renal allograft. 10 living related donors of healthy kidneys served as structural controls. Kidney tissue was taken by needle biopsy at the time of transplantation, either immediately before nephrectomy ($n = 4$) or within 10 min after nephrectomy ($n = 6$). They provided control values for the morphometric and histochemical findings of interest.

Protocol

Each recipient underwent a transplantation procedure and was then immunosuppressed according to a regimen, both of which have been reported in detail elsewhere (4). The protocol called for an examination of each individual on two occasions. The first was intraoperative, $\sim$ 1 h after completion of the vascular anastomosis and reperfusion of the transplanted kidney, at which time a biopsy of the allograft was performed. The second was in the latter part of the first week after transplant. At this time a physiological assessment of the postischemic renal injury was undertaken. In the last 18 patients in this series a histochemical analysis of the inoperative biopsy was undertaken to evaluate the tubule cell cytoskeleton. 10 of these latter patients had a second renal biopsy on day 7 after transplant, so as to evaluate the late morphological and histochemical features of the injury.

Physiological determinations

The inulin clearance according to which transplant recipients were classified into recovering or sustained ARF groups was performed on average on postoperative day 4.4±1.8 (mean±SD). The corresponding clearance determinations in the functional control group were performed between 13 and 60 mo after transplant. A priming dose of inulin (50 mg/kg) was followed by a sustaining infusion calculated to maintain plasma inulin concentration constant at 20 mg/dl. After a 60-min equilibration period, four timed urine collections were made. A blood sample was drawn to bracket each urine collection. Effective GFR was calculated as the average of the four individual inulin clearances. Additional determinations included two indices of tubular function that are widely used in ARF, namely the fractional excretion of sodium and the urine-to-plasma osmolality ratio, and have been described by us in detail previously (4).

The first 19 subjects in the series as well as the functional control group also received an intravenous infusion of a polydisperse preparation of dextran 40 (Rheomacrodex; Pharmacia Fine Chemicals, Uppsala, Sweden), so as to determine the fractional dextran clearance profile. Dextran 40 was administered by bolus in a dose of 130 mg/kg immediately after the inulin prime, and was then infused constantly at half of the rate calculated for inulin. Fractional clearances of dextran (θ_D) were computed using the equation:

$$\theta_D = (U/P)_D / (U/P)_{in} \quad (1)$$

where U/P_D and U/P_{in} refer to the urine-to-plasma concentration ratios of dextran and inulin, respectively. Separation of dextran 40 into narrow fractions ($\sim$ 2 Å radius intervals) was accomplished by elution of urine and plasma from precalibrated, gel permeation columns packed with ultragel ACA 44 (LKB, Pleasant Hills, CA) as described previously (18). The eluted fractions were assayed for dextran concentration using a modification of the autoanalyzer anthrone method of Scott and Melvin (19).

Calculation of fractional inulin backleak (k_{in})

When the permeability properties of the tubule are normal, as is the case in the healthy kidney, all inulin and dextran permeating the glomerular barrier and appearing in the glomerular filtrate should escape reabsorption and reach the final urine. It is the nonreabsorbable nature of these polysaccharide filtration markers that permits estimation of the dextran ultrafiltration characteristics of the glomerular capillary wall (20, 21). For the allograft with postischemic ARF, however, we assume that tubule backleak of inulin (and also dextrans) occurs. If we further assume that such leakage is "passive" (that is, occurs solely by ultrafiltration and/or diffusion through the damaged tubule wall), then the rate of leakage of any such solute should be nearly proportional to the concentration of that solute in the glomerular filtrate. Under such circumstances, the fractional backleak of inulin (defined as the rate of backleak divided by the GFR) will be constant (k_{in}). Precisely the same criteria apply to any dextran species of the ith molecular radius (r_{Di}), leading to a fractional dextran backleak of k_{Di}. However, the permeability of the damaged tubule wall to dextrans would be expected to be a declining function of the size of the dextran molecule: $k_{Di} = f(r_{Di})$; where $k_{Di} \to k_{in}$ as $r_{Di} \to r_{in}$; $k_{Di} \to 0$ as $r_{Di} \to \infty$. Simple mass–balance computations of inulin and dextran cleared by the glomerulus lead to the following relationship (16, 17):

$$\theta_{app} = \theta (1 - k_{Di}) / (1 - k_{in}) = \theta [1 - f(r_{Di})] / (1 - k_{in}) \quad (2)$$

where θ_{app} is the apparent sieving coefficient for the ith dextran based solely on plasma and urine concentration measurements, and θ is the sieving coefficient of the glomerular capillary wall for that dextran. Qualitatively, we can deduce from Eq. 2 that for large dextran molecules where $k_{Di} \approx 0$, $\theta_{app} > \theta$ (since $[1 - k_{in}] > 0$), while for small dextran molecules where $k_{Di} \approx k_{in}$, $\theta_{app} \approx \theta$. Assuming that the dextran sieving characteristics of the glomerular capillary wall in allografts with ARF are the same as those in the control allografts with optimal function, Eq. 2 can be reduced to:

$$\theta_{app}/\theta = (1 - k_{Di}) / (1 - k_{in}) = [1/(1 - k_{in})] - [k_{Di}(1 - k_{in})] \quad (3)$$

where θ now equals the fractional dextran clearance in normal control allografts. Further, k_{in} is a constant for a given subject, whereas k_{Di} is a function of r_{Di}. As $r_{Di} \to r_{in}$, $k_{Di} \to k_{in}$, and as $r_{Di} \to \infty$, $k_{Di} \to 0$. Hence, the ratio (θ_{app}/θ) should increase with r_{Di} from a value of unity (for small r_{Di}) to a limiting value of $1/(1 - k_{in})$ as r increases. Since, as $r_{Di} \to \infty$, $k_{Di} \to 0$, a plot of (θ_{app}/θ) against r should permit a reasonably accurate extrapolation to the limiting value of (θ_{app}/θ) $\to 1/(1 - k_{in})$. This permits calculation of k_{in}. Because k_{in} is the fraction of inulin that leaks back, this value can be used to correct the GFR as measured by urinary inulin clearance (C_{in}) in those with postischemic allograft ARF as follows:

$$\textit{Corrected GFR} = [(1/1 - k_{in}) \cdot C_{in}]. \quad (4)$$

Tubular morphology

Tubules in each biopsy were examined by light and electron microscopy. As described in an earlier paper (4), 1-μm-thick sections of paraffin-embedded tissue were cut and stained with hematoxylin and eosin, and periodic acid-Schiff reagent. An 11 × 11 square grid was inserted into the eye piece of the microscope. Point and intercept counting of seven grid fields at a magnification of 900 was used to calculate the percentage of damaged proximal tubular cells that had exfoliated into the tubule lumen. The cell membrane changes associated with postischemic injury were evaluated by electron microscopy. Intact proximal tubules far from the edge of the biopsy were identified in toluidine blue-stained 0.5-μm-thick sections. Ultrathin sections (60–70 nm) of selected tubules were placed on slotted copper grids and photographed at a final magnification of 5,640. An average of 69 cells per patient (range 37–108) was captured on electron photomi-

crographs and examined. The brush border associated with the apical membrane of each tubule cell was evaluated and classified as normal, diminished, or entirely absent. The frequency of basolateral interdigitations was evaluated by dividing the number of interdigitations emanating from the basal surface by the corresponding length of the tubular basement membrane.

Immunohistochemistry

Antibodies. Affinity-purified rabbit anti–ZO-1 antibody raised against a 69-kD fusion protein corresponding to amino acids 463–1109 of human ZO-1 cDNA was obtained from ZYMED Laboratories, Inc. (South San Francisco, CA) and used at a dilution of 1:10,000. Affinity-purified rabbit polyclonal anti–α-catenin antibody raised against the 15–amino acid carboxy terminal of the α-catenin sequence was kindly provided by Dr. Inke Nathke (Stanford University) and used at a dilution of 1:200. Rabbit polyclonal anti–human β-catenin antibody (YR7) raised against recombinant NH_2-terminal half of human β-catenin was a gift from Dr. David L. Rimm (Yale University, New Haven, CT) and used at a dilution of 1:1,000. Affinity-purified monoclonal antiplakoglobin in mouse ascitic fluid was obtained from BIODESIGN International (Kennebunk, ME) and used at a dilution of 1:5. α_6-integrin distribution was examined with a rat monoclonal antibody, GoH3 (22); GoH3 supernatant was a gift from Dr. Arnoud Sonnenberg at the Netherlands Cancer Institute (Amsterdam, Holland) and was used at a dilution of 1:2. Mouse monoclonal anti–human laminin antibody in 4C7 ascites raised against the A chain of human laminin was obtained from DAKO Corp. (Carpinteria, CA) and used at a dilution of 1:10.

Dual staining with antibodies against Aquaporins 1 and 2 and cytokeratin 8 was used to localize discrete proximal tubules and collecting ducts. Rabbit polyclonal antibodies against Aquaporins were raised against KI-stripped human red blood cell ghosts for Aquaporin 1 (CHIP28) or the carboxy-terminal peptide of rat collecting duct water channel (AQP2, AQP-CD), and were gifts from Dr. Alan S. Verkman (University of California, San Francisco, CA), and used at a dilution of 1:500. Aquaporin 1 and 2 were used as markers for proximal tubule and collecting duct, respectively. Troma-1 rat monoclonal supernatant used to detect cytokeratin K8 was obtained from the National Institutes of Health Developmental Studies Hybridoma Bank (Department of Biology, University of Iowa, under contract NO1-HD-2-3144 from the National Institute of Child Health and Human Development) and was used at a dilution of 1:1. A typical pattern of cytokeratin 8 distribution permitted proximal segments to be distinguished from distal convoluted segments and collecting ducts. In all controls with no ischemia ($n = 4$) and renal allograft recipients ($n = 18$) additional staining was undertaken to ensure that proximal tubule cells from the deep cortex and outer medulla were included in our histochemical analysis. An antibody against Tamm-Horsfall protein from Accurate Chemical and Scientific Corp. (Westbury, NY) was used at 1:200 to identify the medullary segment of the thick ascending limb of Henle's loop (mTAL).

Tissue preparation for immunohistochemistry. A fraction of the tissue obtained from the allograft needle biopsies was immediately dropped into 10 ml of paraformaldehyde-lysine-periodate fixative on ice for 30 min. After fixation, tissue was washed three times in ice-cold PBS. Each wash was carried out for 10 min on ice. After this step, the tissue was cryoprotected by transferring it to a 50-ml conical tube containing 40 ml of 2.5 M sucrose in PBS for at least 48 h at 4°C. Tissue was then immersed in OCT cryoembedding compound (Miles Inc., Kankakee, IL), frozen in liquid N_2, and sectioned or stored at −70°C.

Immunofluorescence staining. The frozen tissue block was mounted onto chucks and sectioned using a 2800 Frigocut N cryostat (Reichert-Jung, Cambridge Instruments, GmbH, Nussloch, Germany). 6-mm-thick sections were transferred onto "subbed" glass slides coated with 0.1% gelatin and 0.01% chromium potassium sulfate. Frozen sections were allowed to warm to room temperature, and were then extracted for 10 min at room temperature with cytoskeleton buffer (50 mM NaCl, 300 mM sucrose, 10 mM piperazine-*N*,*N*′-bis-2-ethane-sulfonic acid, pH 6.8, and 3 mM MgCl, 0.5% Triton X-100, and 1 mM PMSF). Slides were washed twice in PBS at room temperature; each wash was carried out for 10 min. After this step, slides were incubated in blocking solution for 2 h at room temperature in a humidified chamber; the blocking solution consisted of PBS containing 20% normal goat serum, 0.2% BSA, 50 mM NH_4Cl, 25 mM glycine, and 25 mM lysine. Slides were washed twice in PBS containing 0.2% BSA for 10 min at room temperature. Slides were then incubated with the appropriate primary antibody overnight at 4°C in a humidified chamber. Primary antibodies were diluted in PBS containing 20% normal goat serum and 0.2% BSA. For double-labeling experiments, sections were incubated with both primary antibodies. The next day, slides were again washed twice with PBS containing 0.2% BSA, for 10 min at room temperature. Slides were then incubated with the appropriate secondary antibody solutions for 2 h at room temperature in a humidified chamber; for double-labeling experiments, sections were incubated with both secondary antibodies at the same time. Rhodamine- and fluorescein-conjugated secondary antibodies were diluted 1:200 in PBS containing 20% normal goat serum and 0.2% BSA. After the secondary antibody incubation, slides were washed twice in PBS containing 0.2% BSA as above and then mounted with glass coverslips in PBS containing 16.7% Mowiol (Calbiochem Corp., La Jolla, CA), 33% glycerol, and 0.1% paraphenylene diamine. Slides were viewed and photographed using a Zeiss Axioplan epifluorescence microscope equipped with differential interference contrast optics. Photographic slides (Ektachrome ASA 400; Eastman Kodak, Rochester, NY) were used to assess the distribution of each protein. Photographs were taken from at least three different fields for each protein at magnifications of 400, 630, or 1,000.

Statistical analysis

The significance of differences among the two groups and their corresponding control groups was evaluated by ANOVA. In the case of certain demographic and clinical findings, data were available only for the two ARF groups, and the two-way comparison was made using either Student's *t* or Wilcoxon's test, depending on the distribution of the findings. Intrapatient differences in renal morphology in the subset of recipients who had serial biopsies were evaluated by Student's *t* test for paired data. All results are expressed as the mean±1 standard error.

Results

Clinical features. Several characteristics of the allograft recipients are summarized in Table I. The number of patients, their gender distribution, and their age were similar in the groups with sustained versus recovering ARF (Table I). The total time of ischemia (cold storage and rewarming times) was significantly shorter in the recovering than in the sustained ARF

Table I. Characteristics of Patient Population

	Sustained	Recovering
Number of subjects	19	20
Female/Male	8/11	7/13
Age (yr)	49±3	45±2
Cadaveric/Living-related donors	19/0	16/4
Total ischemic time (min)	1464±86	993±128* 1241±77‡
Donor age (yr)	35±4	40±4

Mean±SE. *$P = 0.0046$ vs. sustained ARF; ‡Total ischemic time of allografts excluding four living donor transplants.

Table II. Posttransplant Renal Function

	Sustained	Recovering
Postoperative day	4.9±0.5	4.0±0.4
Inulin clearance (ml/min)	10±2	47±4
Urine flow rate (ml/min)	2.1±0.5	4.2±0.8*
Fractional Na^+ excretion (%)	11.2±3.0	5.0±0.9‡
Urine/plasma osmolality	1.04±0.04	1.01±0.09
Number requiring posttransplant dialysis	12	0
Serum creatinine in those not requiring dialysis (mg/dl)	4.9±1.2	2.0±0.2

Mean±SE. *$P < 0.05$ recovering vs. sustained ARF; ‡$P = 0.07$ recovering vs. sustained ARF.

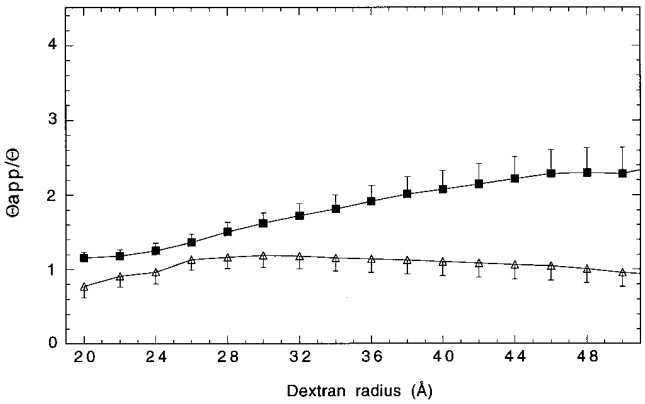

Figure 2. The ratio of fractional dextran clearance in ARF to fractional dextran clearance in control (θapp/θ) is plotted as a function of dextran radius. θapp/θ rises progressively to an asymptotic value of 2.3 in sustained ARF (*filled boxes*). Corresponding values of recovering ARF approximate 1.0 (*open triangles*). Results are mean±SE.

group. However, all four of the living donors in this series donated their kidneys to recipients who went on to exhibit recovering ARF. When these latter donors are excluded, total ischemia time of the remaining cadaveric kidneys did not differ significantly between the sustained and recovering ARF groups: 1464±86 vs. 1241±77 min, respectively (Table I).

Renal function. Physiological evaluation was carried out on an average of 4.9±0.5 d after transplant in the sustained ARF group versus 4.0±0.4 d in the recovering ARF group (Table II). The corresponding inulin clearances were 10±2 and 47±4 ml/min, respectively. Sustained ARF was distinguished from recovering ARF in that the rate of urine flow was lower and the fractional sodium excretion higher (Table II). A urine/plasma osmolality ratio of ~ 1.0 in each group attested to persistent isosthenuria. Of the 19 subjects with sustained ARF, 12 required dialysis postoperatively. In the remaining seven subjects, the serum creatinine level at the time of physiological evaluation was higher than in recovering ARF: 4.9±1.2 vs. 2.0±0.2 mg/dl, respectively (Table II).

The fractional dextran clearance profiles of the groups with sustained and recovering ARF are compared with that of controls with optimally functioning renal allografts in Fig. 1. The fractional dextran clearances are plotted as a function of Einstein-Stokes radius. As shown, the recovering ARF profile tends to be slightly elevated above that in controls, but the difference does not reach significance for any of the narrow dextran fractions that were examined (Fig. 1, *left*). A much more striking disparity is evident between sustained ARF and the controls (Fig. 1, *right*). Fractional dextran clearances in the former are markedly elevated above control over the entire range of molecular radii examined, and the difference achieves statistical significance in the 26–50-Å radius interval. Of note is that fractional dextran clearances in the 18–22-Å radius interval in sustained ARF exceed unity (Fig. 1), a phenomenon that is consistent with proportionately greater backleak of smaller inulin than the larger dextran molecules.

Assuming that the elevation of fractional dextran clearances in sustained ARF is due to disproportionate inulin backleak, we used Eq. 3 to estimate the fraction of filtered inulin that must have leaked back (k_{in}). To do this we plotted the ratio of θ_{app}/θ (fractional clearance in ARF/fractional clearance in control) as a function of molecular radius of the dextran. As shown in Fig. 2, the ratio in sustained ARF rises progressively with increasing radius to an asymptotic limiting value of 2.3, which is equal to $1/(1 - k_{in})$. From the product of the latter and the inulin clearance, we estimate that the true GFR corrected for backleak in sustained ARF is 23 ml/min rather than the 10

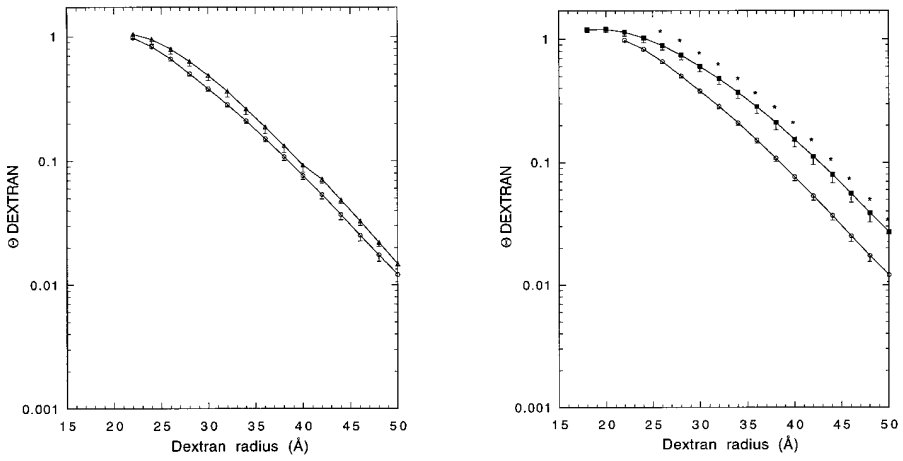

Figure 1. Fractional dextran clearance profiles in recovering (*open triangles, left*) and sustained ARF (*filled squares, right*). Each is compared with control values in optimally functioning renal allografts (*open circles*). Fractional clearances (θ) are plotted as a function of dextran radius. Results are mean±SE. *$P < 0.05$.

Table III. Tubular Morphology of Renal Allografts

	Day 0		Day 7		
	Sustained	Recovering	Sustained	Recovering	Control
Number of subjects	18*	19*	5	5	10
Exfoliated cells (%)	2.8±0.6	2.4±0.4	0.7±0.3‡	0.8±0.3‡	3.0±0.5
Cells with absent brush border (%)	2.6±0.7	1.8±0.7	2.3±1.2	0.8±0.8	3.2±1.1
Cells with decreased brush border (%)	25.2±4.0	21.6±3.4	36.2±7.6	19.3±3.6	20.0±3.7
Basolateral interdigitations (No./mm)	634±86	700±75	731±147	1311±383	864±112

Mean±SE. ‡$P < 0.05$ day 0 vs. day 7; *Biopsy core from one member of each group contained only medulla.

ml/min estimated by the inulin clearance (Table II), and that the fraction of filtered inulin that leaked back was 57%. In contrast to sustained ARF, the θ_{app}/θ ratio for recovering ARF approximates 1.0 over the entire range of molecular radii examined, and does not rise to a limiting value, as was the case in sustained ARF (Fig. 2). This suggests that backleak is not an obvious feature of ARF once it has entered the recovery stage.

Tubule morphology. To determine whether denuded base-

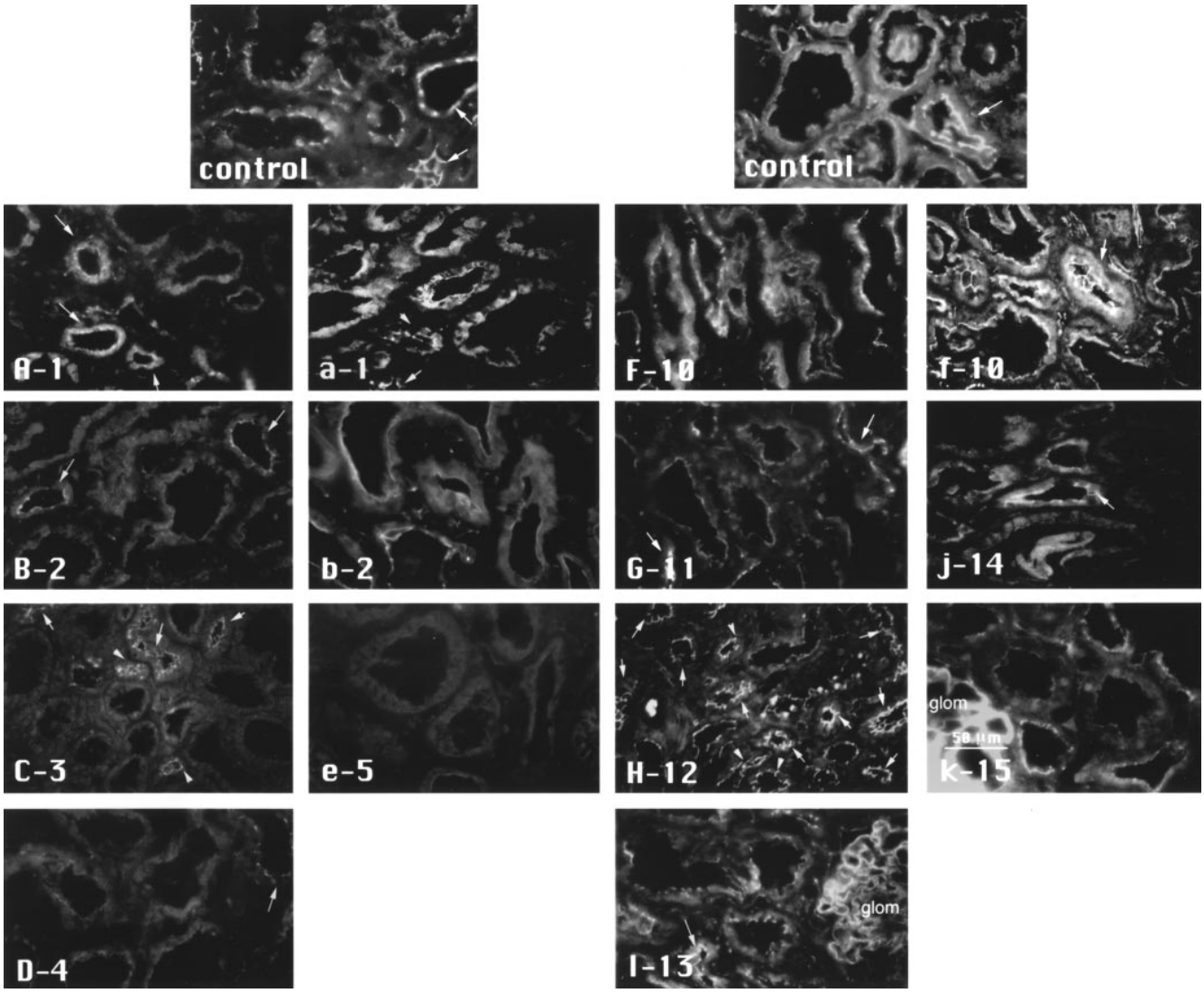

Figure 3. Immunofluorescence microscopy for ZO-1 distribution. The panels in the top row are tissues obtained from prenephrectomy biopsies of living transplant donors (*control*). Panels in the left two columns are representative tissue sections from recipients with sustained ARF. Panels in the right two columns are representative tissues from recipients with recovering ARF. Uppercase letters denote tissues taken after allograft perfusion on the day of transplantation, and lowercase letters denote tissues taken on day 7 after transplant. The same alphabetical letter designates the same patient on a different day. Arrows and arrowheads indicate distal tubules and collecting ducts. Alterations from control in ARF are described in the text.

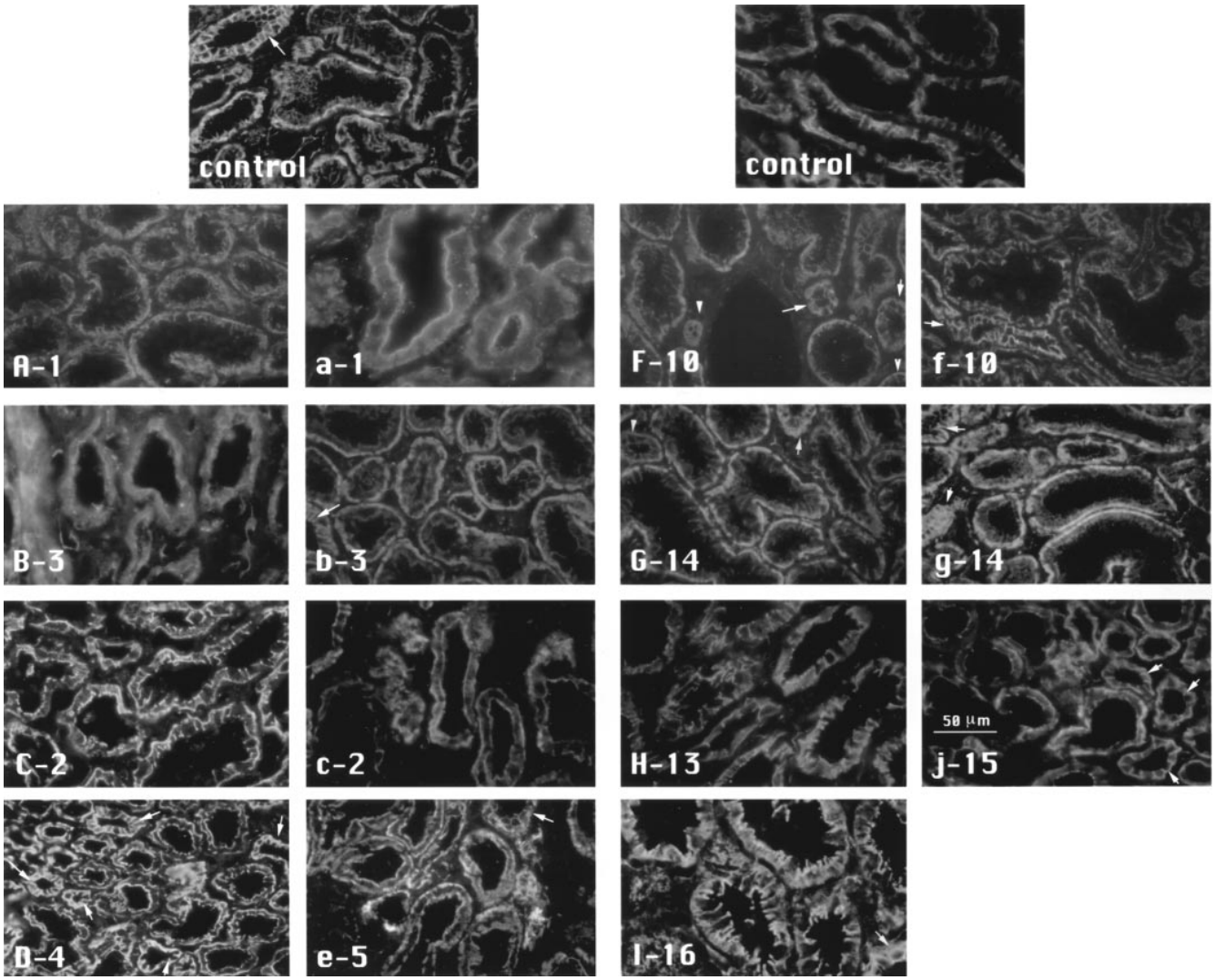

Figure 4. Immunofluorescence microscopy for α-catenin distribution. Panels and symbols are the same as in Fig. 3. Number and letter denoting an individual patient is the same as in Fig. 3. Alterations from control in ARF are described in the text.

ment membrane was an important site of backleak, we examined tubule morphology in paraffin-embedded thick sections and in ultrathin sections using transmission electron microscopy. We estimated the percentage of tubule cells that had exfoliated into the tubule lumen, and this analysis is summarized in Table III. The percentage of exfoliated cells on the transplant day was low among the sustained and recovering ARF groups and the control group, approximating 3% (Table III). Of interest, the percentage of exfoliated cells was even lower in biopsies 7 d after transplant, averaging only 0.7±0.3 and 0.8±0.3% in sustained and recovering ARF, respectively. The latter values were not significantly different from each other, but each value was significantly lower by paired *t* test than the corresponding transplant day value.

The ultrastructural appearance of proximal tubule cells was also similar in the sustained and recovering ARF groups on the transplant day. The percentage of cells with absent or diminished apical brush border was higher, and the frequency of basolateral interdigitations was lower in sustained than in recovering ARF, both on the transplant day and on day 7 after transplant, but the differences failed to achieve statistical significance (Table III). We note with interest that during the course of examining 2,196 tubule cells by electron microscopy, we observed only five examples of denudation of the underlying tubule basement membrane in four recipients with sustained ARF on the day of transplantation. The corresponding number in 613 control cells was one example of denudation. We infer that any tubule cell exfoliation at these sites must have been rapidly followed by spreading of adjacent cells, so as to cover the exposed basement membrane.

Immunohistochemistry. Staining for Tamm-Horsfall protein confirmed the presence of medullary tubule cells of the thick ascending limb of Henle in 80% of the biopsies examined. Given the presence of medullary tissue, we infer that CHIP 28 positive proximal tubule cells included those of the pars recta, S3 segment of this structure. Staining patterns for each protein examined in each functional group varied among individuals and among cells. This heterogeneity was more pronounced in the intraoperative biopsies taken after allograft reperfusion, compared with the repeat biopsies on day 7 after

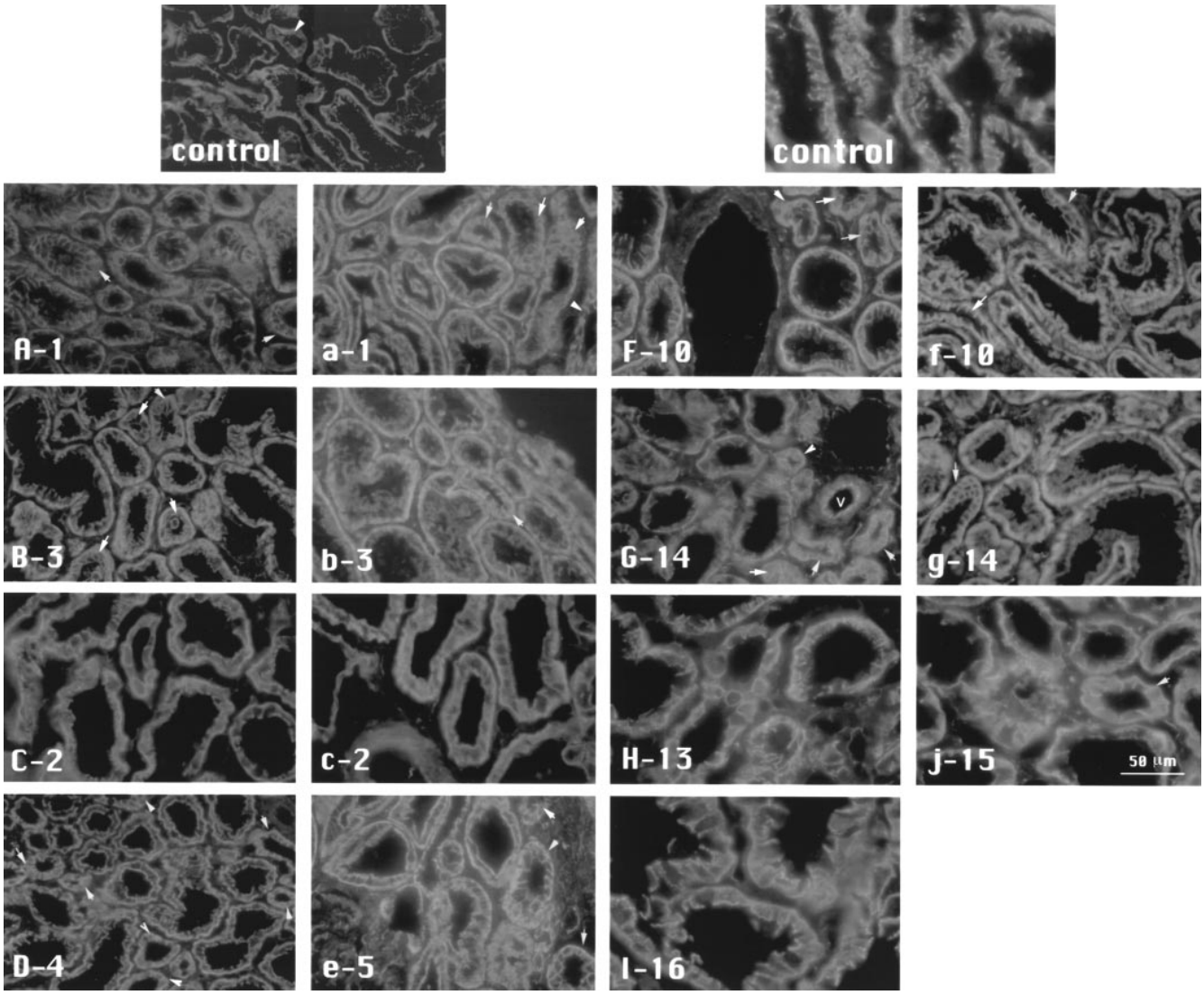

Figure 5. Immunofluorescence microscopy of β-catenin distribution. Panels and symbols are the same as in Fig. 3. Number and lettering denoting an individual patient is the same as in Fig. 4. Alterations from control in ARF are described in the text.

transplant. The subcellular distribution of proteins in proximal tubule cells was substantially different between groups. Differences in staining patterns in distal tubule cells between groups were not as marked as those in proximal tubule cells. Control tissues showed a consistent pattern of protein distributions for each segment of the nephron. Figs. 3–6 show representative staining patterns for three proteins: a tight junction cytoplasmic protein (ZO-1; Fig. 3), α-catenin (Fig. 4), and β-catenin (Fig. 5), cytoplasmic proteins associated with adherens junctions, and α6-integrin, a receptor for the extracellular matrix protein laminin and laminin itself (Fig. 6).

Distribution of tight junction protein ZO-1 (Fig. 3). In control tissue sections obtained from prenephrectomy biopsies of living transplant donors, ZO-1 is localized to the apical intercellular junctional complex in all renal tubular epithelial cells although some diffuse background staining is also detected in cells. In full cross-sections of tubules, ZO-1 staining appears as individual puncta close to the luminal surface of cells, as expected for the location of the tight junction. Proximal tubule cells show a fine punctate staining along the luminal surface in tangential sections. The intensity of ZO-1 staining is stronger and more distinct in distal tubules and collecting ducts (arrows or arrowheads) than in proximal tubule cells. In tissues obtained from recipients with sustained ARF taken after allograft perfusion on the day of transplantation (Fig. 3, *A, B, C,* and *D*), ZO-1 staining of the apical intercellular junctional complex is substantially less prominent in proximal tubule cells compared with control staining. Note, however, that distal tubule cells in this group show ZO-1 staining at the apical intercellular junction which is similar in distribution and intensity to that in control tissue. Similar findings were obtained in 8 out of 10 cases in the sustained ARF group. The remaining two cases show a more normal staining pattern similar to that in controls. In tissues obtained from recipients with sustained ARF taken on day 7 after transplant (Fig. 3, *a*, *b*, and *e*), ZO-1 staining shows a subcellular pattern and intensity similar to that on the

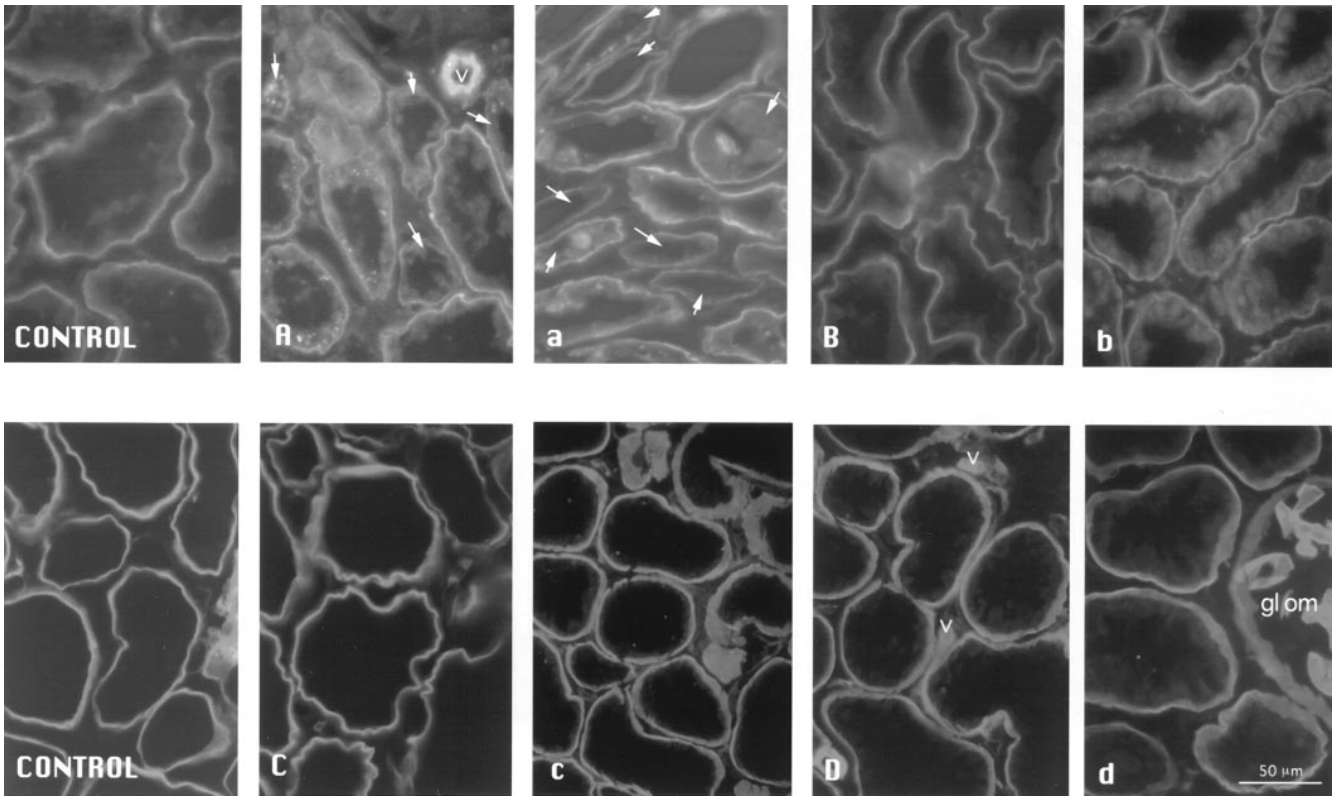

Figure 6. Immunofluorescence microscopy for α6-integrin (*top*) and laminin (*bottom*). The two left panels are from control subjects. *A*, *a*, *C*, and *c* are from the recipients with sustained ARF. *B*, *b*, *D*, and *d* are from the recipients with recovering ARF on the day of transplantation (*upper-case letters*) or day 7 after transplant (*lowercase letters*), respectively. V denotes blood vessel, all other symbols and abbreviations are the same as in Fig. 3. Alterations from control in ARF are described in the text.

day of transplantation. Note, however, that one patient (Fig. 3 *b*) shows linear staining for ZO-1 on the apical (luminal) membrane of proximal tubule cells.

Tissues obtained intraoperatively after allograft perfusion from recipients destined to have recovering graft function (Fig. 3, *F*, *G*, *H*, and *I*) show apical intercellular junctional staining for ZO-1 in proximal tubule cells although the intensity is not as strong as that in the control. In these recipients, the ZO-1 staining pattern in distal tubule cells is similar in intensity and distribution as that in the control. Five out of six cases had these staining patterns for ZO-1 in proximal and distal tubule cells. Tissues obtained from recipients with recovering renal function on day 7 after transplant (Fig. 3, *f* and *k*) show apical intercellular junctional staining for ZO-1 in proximal tubule cells that is stronger in intensity than that on the day of transplantation. However, one case (Fig. 3 *j*) shows less prominent staining for ZO-1 in proximal tubule cells. Distal tubule cells in all cases show apical intercellular junctional staining for ZO-1 similar to that in the control.

Distributions of α-catenin and β-catenin (Figs. 4 and 5). The distributions in control tubules of α- and β-catenin and plakoglobin (γ-catenin) were essentially identical. Deviations from normal in the two ARF groups were also similar for each catenin. Accordingly, we will use α-catenin and β-catenin as a representation for all three proteins.

In control tissues, staining for α-catenin and β-catenin is localized to the basolateral membrane of cells of the proximal and distal tubules. The pattern of α-catenin and β-catenin staining in proximal tubule cells frequently appears as a stringy or serpiginous pattern which corresponds to a tangential view of lateral membrane interdigitation.

Very similar distributions of α-catenin (Fig. 4) and β-catenin (Fig. 5) were detected in patients with sustained ARF and recovering graft function. Results are described in detail for α-catenin. In tissues obtained from recipients with sustained ARF on the day of transplantation (Fig. 4, *A*, *B*, *C*, and *D*), the intensity of α-catenin staining of proximal tubule cells is less compared with that in controls, especially along the lateral membrane. Occasionally, we note an accentuation of α-catenin staining of the apical end of the lateral membrane (Fig. 4, *C* and *D*), and redistribution of some α-catenin staining to the apical membrane (Fig. 4 *D*), a finding that was confirmed by deconvolution optical sections (data not shown). Distal tubule cells exhibit strong basolateral membrane staining for α-catenin similar to that of the control. In proximal tubule cells of recipients with sustained ARF on day 7 after transplant (Fig. 4, *a*, *b*, *c*, and *e*), the diminution of α-catenin staining associated with lateral membranes and de novo staining of apical membranes are more pronounced than on the transplant day. One case also shows diminished basal membrane staining for α-catenin (Fig. 4 *a*). The other three cases show intense basal membrane staining, which together with apical membrane staining

gives the appearance of a "tram track" (Fig. 4, *b*, *c*, and *e*). Distal tubule cells continue to show only strong basolateral membrane staining of α-catenin.

In tissues obtained from recipients destined to have recovering graft function on the day of transplantation (Fig. 4, *F*, *G*, *H*, and *I*), α-catenin staining is localized to the basolateral membrane in proximal tubule, distal tubule, and collecting duct cells in all six cases studied. We noticed strong basal membrane staining in two cases (Fig. 4, *F* and *G*) and strong lateral membrane staining in the other two cases (Fig. 4, *H* and *I*). One case shows accentuation of α-catenin staining on the lateral membrane towards the luminal side (Fig. 4 *I*). Distal tubule cells continue to show distinct basolateral membrane staining for α-catenin similar to that of the control. In tissue obtained from one of the recipients with recovering graft function on day 7 after transplant, α-catenin staining is more intense than on the day of transplantation (Fig. 4 *f*). Another case shows almost the same pattern of α-catenin staining as that on the day of transplantation (Fig. 4 *g*). The third case shows strong basolateral membrane staining of α-catenin similar to that in the control (Fig. 4 *j*). Distal tubule cells show strong basolateral membrane staining for α-catenin similar to that in controls.

As was the case for α-catenin, the staining for β-catenin of proximal, but not distal tubule cells in allografts differed from control; more so in sustained than recovering ARF (Fig. 5). Staining was less intense especially along the lateral membrane on day 0 (Fig. 5, *A–D*). De novo staining of the apical membrane with tram tracking was also observed, both on day 0 (*C-2*, *D-4*, Fig. 5) and on day 7 (*a-1*, *c-2*, *e-5*, Fig. 5).

Distributions of α6-integrin and laminin (Fig. 6). In control tissues, proximal and distal tubule cells and collecting duct cells exhibit continuous basal membrane staining for α6-integrin. A pattern of continuous and predominantly basal membrane staining for α6-integrin, similar to that of controls, is observed in recipients of both ARF groups on the day of transplantation and day 7 after transplant. In addition, cytoplasmic aggregates of α6-integrin staining in proximal tubule cells are detectable in recipients with sustained ARF, both on the day of transplantation and on day 7 after transplant (Fig. 6, *A* and *a*). In control tissue, strong basal membrane staining for laminin is detected in cells in all segments of the nephron. A pattern of basal membrane staining indistinguishable from the control is observed in recipients of both ARF groups on the day of transplantation and day 7 after transplant (Fig. 6).

Discussion

Previously, we have shown that transplantation of a cadaveric renal allograft is almost always followed by postischemic injury (4). In clinical practice, such injury is classified into two grades according to the rapidity with which the freshly allografted kidney achieves an adequate clearance of nitrogenous waste products. Recipients with rapid resolution of azotemia are designated as exhibiting "prompt graft function," and correspond to the group classified as recovering ARF in this study. Those who fail to recover adequate renal function in the first week after transplant are described as having "delayed graft function" and correspond to the group classified as sustained ARF in this study. Members of the latter group were distinguished from the former by virtue of a severely depressed inulin clearance. Additional differences included greater fractional sodium excretion and more disruption of tubule cell cytoskeletons, notably those of the proximal tubule. Sustained ARF was also distinguished from recovering ARF in that the former exhibited marked elevation of the fractional dextran clearance profile, a phenomenon that is consistent with transtubular backleak of filtrate (16, 17).

Elevation of fractional dextran clearances is in fact not pathognomonic of backleak. A selective reduction in either the glomerular perfusion rate or pressure, both of which are likely to eventuate in postischemic ARF, is predicted to elevate fractional dextran clearances (23). However, this effect is marked only for relatively permeant dextrans of radius ≤ 30 Å (23). Conversely, the loss of glomerular size-selectivity that accompanies heavy proteinuria is a consequence of isolated defects that occupy only a minor fraction of the filtration barrier. As a result, the enhancement of fractional clearances is selective for nearly impermeant dextran molecules of radius ≥ 50 Å (24). Thus, neither of the aforementioned alterations can explain satisfactorily the uniform elevation of fractional clearance over the broad size range of dextran molecules observed in this study. Particularly suggestive of backleak is that fractional clearance of dextrans in the 18–22-Å interval exceeded unity (Fig. 1). Since filtrate is formed by passive forces, there is no conceivable circumstance under which a larger dextran molecule can be filtered more rapidly than a smaller inulin molecule (radius 14–16 Å). Therefore, a plausible explanation for the finding is that postischemic damage to the tubule results in a size-dependent backleak of inert polysaccharides to which the tubule is normally impermeable. Under this circumstance, smaller inulin molecules would be expected to leak back with greater facility than larger dextran molecules. An ensuing decline in the final urine/plasma ratio, which is more marked for inulin than dextran, would then result in an "apparent" elevation of fractional dextran clearances (Eq. 1).

Also suggestive of a size-dependent transtubular backleak is the finding that the disparity between fractional dextran clearances in sustained ARF and controls grows progressively larger in the radius interval 22–44 Å, and then becomes constant for radii > 44 Å (Fig. 2). Such constancy suggests that the damaged tubule wall progressively restricts dextran molecules on the basis of their size and eventually becomes completely impermeable to molecules of $>$ 44-Å radius. We compute that 57% of filtered inulin must have leaked back to explain the observed elevation of the fractional dextran clearance profile in sustained ARF. This is similar in magnitude to what has been found by micropuncture or microperfusion of tubules in rats with postischemic ARF (7, 8). It is also similar to our earlier estimates of backleak in other forms of human postischemic ARF, using the same dextran fractional clearance technique (16, 17, 25). Correcting the observed inulin clearance for fractional inulin backleak, we calculate that the "actual" GFR in sustained ARF was only 23 ml/min. Thus, backleak of filtrate per se makes only a modest contribution to the profound reduction of GFR that is associated with postischemic ARF.

In attempting to elucidate a structural basis for backleak, we have examined a possible role for denuded tubule basement membrane. In vitro studies of this extracellular matrix have shown it to have a high hydraulic permeability and also to be relatively more permeable to dextran macromolecules than for example, the glomerular capillary wall (26). Exposure of this structure to tubule fluid as a result of exfoliation of the overlying tubule cells could thus account for the phenomenon

of backleak. The present study does not provide any evidence to support this potential portal of entry into the interstitium for tubule fluid, however. In keeping with earlier studies of postischemic ARF by ourselves and others (4, 27–32), we found the prevalence of tubule cell exfoliation in the sustained ARF group to be low, and not different from that in either the control or recovering ARF groups. The reason for the finding that 3% of tubule cells have exfoliated into the lumen in our living donor control group is obscure. We speculate that handling of the donor kidney and the vascular pedicle before nephrectomy results in sufficient ischemic injury to account for this observation (5). We also note with interest that both on the day of transplant and on day 7 after transplant, we rarely observed an exposed segment of tubule basement membrane among the thousands of tubule cells that we examined by light or electron microscopy. It seems feasible that surviving cells adjacent to a site of exfoliation spread promptly to cover the underlying basement membrane, thereby reforming a continuous monolayer of cells.

The remainder of our structural analysis was directed to exploring the possibility of a paracellular pathway for backleak by examining the subcellular distribution of the zonula occludens and adherens protein complex. We found abnormalities of the zonula occludens protein, ZO-1, which is an essential structural component of intercellular tight junctions (33). In addition to a reduction in staining intensity, the distribution of ZO-1 was altered occasionally in sustained ARF. Rather than localization at the lateral borders of the apical membrane where tight junctions should form, staining for ZO-1 was diffusely present along the apical membrane. We also observed abnormalities in the distribution of adhesion complexes comprising α, β, and γ-catenin, which are structurally required to maintain cadherin-mediated cell–cell adhesion (34, 35). Instead of normal distributions with concentration at the apical end of the lateral membrane, staining for all three catenins was markedly diminished in sustained ARF. Furthermore, we observed a redistribution of catenins to the apical membrane. Although observed alterations in the histochemical appearance of the membrane-associated proteins were heterogenous, both between individual cells of a given recipient and between recipients, they tended to be more marked in sustained than recovering ARF, to persist on day 7 after transplant, and to be largely confined to cells of the proximal rather than the distal tubule.

Unfortunately, we were not able to examine the distribution of cadherin(s) in these patients. Although we tested a variety of antibodies, none was found to give consistent staining in control tissue. Nevertheless, previous studies have shown that the cellular and subcellular patterns of cadherin and catenin staining along the nephron are identical (36). Therefore, we suspect a similar alteration of cadherin distribution along damaged proximal tubule cells to that observed by us for catenins. At present, the mechanism(s) involved in disruption of ZO-1 (tight junction) and catenin (adherens junction) distributions are unknown. However, given the requirement for cadherin-mediated adhesion for tight junction assembly and maintenance (37), and the integral role of the actin cytoskeleton in adhesion, we suggest that disruption of tight junctions may be a consequence of disorganization of the actin cytoskeleton (37, 38). The ensuing effects on cadherin-mediated cell–cell adhesion, in turn, could result in the development of a proximal tubule paracellular pathway. It is also possible that the tight junction may be a direct target of damage and that loss of structural integrity of the tight junction results in diffusion of cadherin–catenin complexes from the lateral to the apical membrane. Another possibility is that the organization of the tight junction integral membranous protein, occludin (39), might be altered, but further studies are needed to examine this possibility. Nevertheless, the above findings are consistent with disturbed gate and fence functions of the tight junction and cell–cell adhesion caused by ischemic injury to the tubules (11, 15). We suggest that impaired gate function provides an explanation for the evidence supporting transtubular backleak in these patients, while impaired fence function accounts for the apical redistribution of the catenins.

Studies of tubule cell monolayers in culture have been interpreted to indicate that another class of adhesion molecule, the integrins, is redistributed to the apical membrane as a result of postischemic injury (12–14). We were unable to confirm such redistribution in the postischemic kidneys of this study. However, we wish to emphasize that whereas the previous studies examined α_3, α_4, α_v, β_1, and β_3 subunits of integrins we examined α6-integrin, which is the receptor for laminin. The absence of changes in the intensity and distribution of staining for α6-integrin and laminin in the sustained ARF group in this study suggests that at least this cell–extracellular matrix interaction was normal. Preservation of the latter function in postischemic injury to the renal allograft could explain the paucity of tubule cell exfoliation and basement membrane denudation, when compared with experimental postischemic ARF in the rat.

We conclude that impairment of both tight junctions and cell–cell adhesion along the lateral membrane of proximal tubule cells provides a paracellular pathway for backleakage of filtrate in the sustained form of ARF in the renal allograft. The lack of evidence of tubule cell exfoliation in this form of postischemic injury points away from denuded tubular basement membrane as an important site of backleak. Appropriate basal membrane distribution of the laminin receptor, α6-integrin, might be important in preserving cell–substratum adhesion and might account for the sparse exfoliation that we observed. Regardless of the precise pathway that filtrate follows from tubule lumen to interstitium, we compute that the contribution of backleak to depression of GFR in this form of postischemic ARF is a modest one, and that changes in other GFR determinants must be invoked to explain the observed level of hypofiltration.

Acknowledgments

This study was supported by grants R01 DK-50712 and M01-RR00070 from the National Institutes of Health. Dr. Kwon's postdoctoral fellowship was supported by the Satellite Dialysis Centers Fund in Nephrology.

References

1. Arendhorst, W.J., W.F. Finn, and C.W. Gottschalk. 1976. Micropuncture study of acute renal failure following temporary renal ischemia in the rat. *Kidney Int.* 10(Suppl. 6):S100–S105.

2. Tanner, G.A., and S. Sophasan. 1976. Kidney pressures after temporary renal artery occlusion in the rat. *Am. J. Physiol.* 230:1173–1181.

3. Burke, T.J., R.E. Cronin, K.L. Duchin, L.N. Peterson, and R.W. Schrier. 1980. Ischemia and tubule obstruction during acute renal failure in dogs: mannitol in protection. *Am. J. Physiol.* 238:F305–F314.

4. Alejandro, V., J.D. Scandling, R.K. Sibley, D. Dafoe, E. Alfrey, W.M. Deen, and B.D. Myers. 1995. Mechanisms of filtration failure during post-

ischemic injury of the human kidney. A study of the reperfused renal allograft. *J. Clin. Invest.* 95:820–831.

5. Myers, B.D., C. Miller, J. Mehigan, C. Olcott, H. Golbetz, C.R. Robertson, G. Derby, R. Spencer, and S. Friedman. 1984. Nature of the renal injury following total renal ischemia in man. *J. Clin. Invest.* 73:329–341.

6. Myers, B.D. 1996. Pathogenetic processes in human acute renal failure. *Semin. Dialysis.* 9:444–453.

7. Hanley, M.J., and K. Davidson. 1981. Prior mannitol and furosemide infusion in a model of ischemic acute renal failure. *Am. J. Physiol.* 241:F556–F564.

8. Eisenbach, G.M., and M. Steinhausen. 1973. Micropuncture studies after temporary ischemia of rat kidneys. *Pfluger's Arch.* 343:11–25.

9. Yagil, Y., B.D. Myers, and R.L. Jamison. 1988. Course and pathogenesis of postischemic acute renal failure in the rat. *Am. J. Physiol.* 24:F257–F264.

10. Molitoris, B.A., S.A. Falk, and R.H. Dahl. 1989. Ischemia-induced loss of epithelial polarity. Role of the tight junction. *J. Clin. Invest.* 84:1334–1339.

11. Molitoris, B.A. 1991. Ischemia-induced loss of epithelial polarity: potential role of the actin cytoskeleton. *Am. J. Physiol.* 260:F769–F778.

12. Goligorsky, M.S., W. Lieberthal, L. Racusen, and E.E. Simon. 1993. Integrin receptors in renal tubular epithelium: new insights into pathophysiology of acute renal failure. *Am. J. Physiol.* 264:F1–F8.

13. Noiri, E., V. Romanov, T. Forest, J. Gailit, G.F. DiBona, F. Miller, P. Som, Z.H. Oster, and M.S. Goligorsky. 1995. Pathophysiology of renal tubular obstruction: therapeutic role of synthetic RGD peptides in acute renal failure. *Kidney Int.* 48:1375–1385.

14. Lieberthal, W., J.B. Mckenney, C.R. Kiefer, L.M. Synder, V.M. Kroshian, and M.D. Sjaastad. 1997. β1 integrin-mediated adhesion between renal tubular cells after anoxic injury. *J. Am. Soc. Nephrol.* 8:175–183.

15. Mandel, L.J., R. Bacallao, and G. Zampighi. 1993. Uncoupling of the molecular "fence" and paracellular "gate" functions in epithelial tight junctions. *Nature.* 361:552–555.

16. Moran, S.M., and B.D. Myers. 1985. Pathophysiology of protracted acute renal failure in man. *J. Clin. Invest.* 76:1440–1448.

17. Myers, B.D., R. Chui, M. Hilberman, and A.S. Michaels. 1979. Transtubular leakage of glomerular filtrate in human acute renal failure. *Am. J. Physiol.* 237:F319–F325.

18. Granath, K.A., and B.E. Kvist. 1967. Molecular weight distribution analysis by gel chromatography on Sephadex. *J. Chromatography.* 28:69–81.

19. Scott, T.A., and E.H. Melvin. 1953. Determination of dextran with anthrone. *Anal. Chem.* 25:1656–1661.

20. Chang, R.L.S., I.F. Ueki, J.L. Troy, W.M. Deen, C.R. Robertson, and B.M. Brenner. 1975. Permselectivity of the glomerular capillary wall to macromolecules. II. Experimental studies in the rats using neutral dextran. *Biophys. J.* 15:887–906.

21. Chang, R.L.S., C.R. Robertson, W.M. Deen, and B.M. Brenner. 1975. Permselectivity of the glomerular capillary wall to macromolecules. I. Theoretical considerations. *Biophys. J.* 15:861–886.

22. Sonnenberg, A., H. Daams, M.A. Van der Valk, J. Hilkens, and J. Hilgers. 1986. Development of mouse mammary gland: identification of stages in differentiation of luminal and myoepithelial cells using monoclonal antibodies and polyvalent antiserum against keratin. *J. Histochem. Cytochem.* 34:1037–1046.

23. Brenner, B.M., M.P. Bohrer, C. Baylis, and W.M. Deen. 1977. Determinants of glomerular permselectivity: insights derived from observations in vivo. *Kidney Int.* 12:229–237.

24. Deen, W.M., C.R. Bridges, B.M. Brenner, and B.D. Myers. 1985. A heteroporous model of size-selectivity: application to normal and nephrotic humans. *Am. J. Physiol.* 249:F374–F389.

25. Myers, B.D., B. Carrie, R.R. Yee, M. Hilberman, and A.S. Michaels. 1980. Pathophysiology of hemodynamically-mediated acute renal failure in man. *Kidney Int.* 18:495–504.

26. Daniels, B.S., E.B. Hauser, W.M. Deen, and T.H. Hostetter. 1992. Glomerular basement membrane: in vitro studies of water and protein permeability. *Am. J. Physiol.* 262:F919–F926.

27. Olsen, T.S., H.S. Olsen, and H.E. Hansen. 1985. Tubular ultrastructure in acute renal failure in man: epithelial necrosis and regeneration. *Virchows Arch. (Pathol. Anat.).* 406:75–89.

28. Jones, D.B. 1982. Ultrastructure of human acute renal failure. *Lab. Invest.* 46:254–264.

29. Solez, K., L. Morel-Maroger, and J.D. Sraer. 1979. The morphology of "acute tubular necrosis" in man: analysis of 57 renal biopsies and a comparison with glycerol model. *Medicine (Baltimore).* 58:362–376.

30. Solez, K. 1983. Pathogenesis of acute renal failure. *Int. Rev. Exp. Pathol.* 24:277–328.

31. Trump, B.F., I.K. Berezesky, and R.A. Cowley. 1982. The cellular and subcellular characteristics of acute and chronic injury with emphasis on the role of calcium. *In* Pathophysiology of Shock, Anoxia, and Ischemia. R.A. Cowley and B.E. Trump, editors. Williams & Wilkins, Baltimore. 6–46.

32. Solez, K., L.C. Racusen, N. Marcussen, I. Slatnik, I. Keown, J-F. Burdick, and S. Olsen. 1993. Morphology of ischemic acute renal failure, normal function, and cyclosporine toxicity in cyclosporine-treated renal allograft recipients. *Kidney Int.* 43:1058–1067.

33. Furuse, M., M. Itoh, T. Hirase, A. Nagafuchi, S. Yonemura, S. Tsukita, and S. Tsukita. 1994. Direct association between occludin and ZO-1 and its possible involvement in the localization of occludin at tight junctions. *J. Cell Biol.* 127:1617–1626.

34. Ozawa, M., H. Baribault, and R. Kemler. 1989. The cytoplasmic domain of the cell adhesion molecule uvomorulin associates with three independent proteins structurally related in different species. *EMBO (Eur. Mol. Biol. Organ.) J.* 8:1711–1719.

35. Nagafuchi, A., and M. Takeichi. 1988. Cell binding function of E-cadherin is regulated by the cytoplasmic domain. *EMBO (Eur. Mol. Biol. Organ.) J.* 7:3679–3684.

36. Piepenhagen, P.A., and W.J. Nelson. 1995. Differential expression of cell-cell and cell-substratum adhesion proteins along the kidney nephron. *Am. J. Physiol.* 269:C1433–C1449.

37. Gumbiner, B. 1996. Cell adhesion: the molecular basis of tissue architecture and morphogenesis. *Cell.* 84:345–357.

38. Bacallao, R., A. Garfinkel, S. Monke, G. Zampighi, and L.J. Mandel. 1994. ATP depletion: a novel method to study junctional properties in epithelial tissues. I. Rearrangement of the actin cytoskeleton. *J. Cell Sci.* 107:3301–3313.

39. Furuse, M., T. Hirase, M. Itoh, A. Nagatuchi, S. Yonemura, and S. Tsukita. 1993. Occludin: a novel integral membrane protein localizing at tight junctions. *J. Cell Biol.* 103:1777–1788.